Proceedings of ASME Turbo Expo 2011
GT2011
June 6-10, 2011, Vancouver, British Columbia, Canada

GT2011-46435

ELEMENTS OF DYNAMIC CHARACTERIZATION OF A BLADED DISK BY USING THE TIP-TIMING METHOD UNDER VACUUM CONDITIONS

Vsevolod Kharyton *
Laboratory of Tribology and System Dynamics
UMR CNRS 5513, Ecole Centrale de Lyon
36 av. Guy de Collongue, 69134 Ecully Cedex, France
vsevolod.kharyton@ec-lyon.fr

Claude Gibert
Laboratory of Tribology and System Dynamics
UMR CNRS 5513, Ecole Centrale de Lyon
36 av. Guy de Collongue, 69134 Ecully Cedex, France
claude.gibert@ec-lyon.fr

Laurent Blanc
Laboratory of Tribology and System Dynamics
UMR CNRS 5513, Ecole Centrale de Lyon
36 av. Guy de Collongue, 69134 Ecully Cedex, France
laurent.blanc@ec-lyon.fr

Fabrice Thouverez
Laboratory of Tribology and System Dynamics
UMR CNRS 5513, Ecole Centrale de Lyon
36 av. Guy de Collongue, 69134 Ecully Cedex, France
fabrice.thouverez@ec-lyon.fr

ABSTRACT

This article describes the process of identifying the dynamic properties of a blisk by noncontact measurements provided by the tip-timing method. Attention is focused on tip-timing measurements for mode identification in the presence of the Coriolis effect.

Firstly, the standing wave response is studied by using tip-timing measurements that provide the amplitude and phase distributions of each blade over a fixed measurement period for identifying the number of nodal diameters of the mode. Secondly, the travelling wave response is identified, followed by the calculation of the frequency response of the blisk, in order to derive the damping ratios. As the mode considered is found in the domain of strong disk-to-blade coupling, it could be subject to the Coriolis effect. Blade tip-timing (BTT) measurements were used to reveal that the mode was split into forward and backward modes with respect to blisk rotation.

All the results obtained after processing the tip-timing measurements are compared with data from the strain gauges with which only a few blades were equipped. The correlation of deformations measured by the strain gauges and blade tip tangential displacement obtained through tip-timing measurements is performed by using realistic finite element models of the blisk.

Key words: tip-timing method, travelling wave, mode identification, Coriolis effect, bladed disk, forced response

1. INTRODUCTION

The main advantage of the blade tip-timing (BTT) method is that it makes full and contactless monitoring of blade vibration possible even when using only one sensor, contrary to strain gauges. Monitoring the health of aviation engines requires relevant information about blade vibrations. Thus the BTT method can be used to develop a relatively non intrusive and on-line system for monitoring the dynamic performance of the blade in operation. Different methodologies are used to provide tip-timing measurements under either synchronous or asynchronous vibration, emphasizing the undersampled nature of such measurements [1]. As reported in [2], such data processing methods show dependency between the number of probes and the frequency content of the vibration signal. Single-probe measurements are described in [3], stressing the angular position of the probe and its influence on errors of maximum amplitude reconstruction. Questions concerning the correlation between vibration amplitude measured by probe and blade tip displacement require consideration [4]. A recent study [5] described a methodology for performing multi-probe measurements for mode shape reconstruction and the possible identification of cracks in blades. A minimum of two probes are required to perform this reconstruction for each measurement. Most of the studies mentioned assume synchronous vibration and constant rotation speed during one measurement (rotation period).

The specific excitation tools equipping the test rig used in this study allow controlling asynchronous excitation. Thus excitation is known exactly, unlike flutter conditions or channel

* Author for correspondence

irregularities which are real sources of asynchronous vibrations in engines. Moreover, using these tools is not dangerous for the structure and the experiment can be focused on the specific mode chosen.

Here, the asynchronous vibration of a bladed disk is investigated in order to demonstrate the applicability of single-probe measurements for mode type (nodal diameter number, travelling or standing wave response, damping ratio) identification. Therefore, the study is structured according to three main tasks:

(1) Tip-timing measurements on a realistic bladed disk
(2) The identification of mode shapes for two types of response: standing wave response and travelling wave response
(3) The calculation of the modal damping ratio and comparison of BTT results with results from strain gauge data.

Strictly speaking, no modal extraction method that would result in a mode shape is applied here and only operating deflection shapes (ODS) are analyzed at resonances. However, since the latter are well separated and damping is light, ODS are believed to be close to modal shapes.

2. TIP-TIMING DATA PROCESSING FOR MODE IDENTIFICATION

The excitation on the test rig used in the study is sinusoidal, of known frequency and asynchronous with regard to rotation speed. Thus greater flexibility in terms of operation of the blisk in vibratory state is possible, especially with respect to the calculation of vibration amplitude directly from single probe data. Consequently, data processing approaches have to be developed and applied to experimental tip-timing measurements.

Fig. 1 Blade tip-timing method configuration (1…3 – probes) shows the diagram of tip-timing probe locations. Three probes were used, all installed on the tip profile of the blade leading edge. Measurement data synchronization was ensured by a once per revolution (OPR) sensor emitting an impulse once per blisk rotation. Using the sensor allowed linking the blades to their reference numbers during the tip-timing measurements.

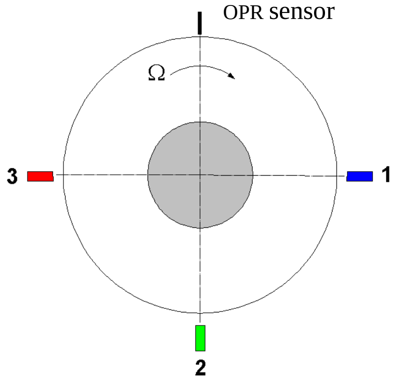

Fig. 1 Blade tip-timing method configuration (1…3 – probes)

Blade tip response has l data points at every rotation. A tip response is assumed to be sinusoidal and mono-harmonic, hence it can be expressed as follows [5]:

$$a_p^j = A^j \sin(\omega t_p^j + \psi^j),\ j = 1 \ldots n_r,\ p = 1 \ldots l\,, \qquad (1)$$

where ω is the frequency of vibration, A^j is the maximum amplitude of j-th blade tip and ψ^j is the phase, t_p^j is the time of arrival of the j-th blade tip at the p-th probe, n_r is the number of blades (36 in our case), l is the number of probes.

In the case of three probes (Fig. 1), equation (1) leads to a system of three equations (over-determined) with the unknowns A and ψ. For a blade at a particular measurement point (given rotation) the system is written as:

$$\begin{cases} A^j \sin(\omega t_1^j + \psi^j) = b^j \cos(\omega t_1^j) + c^j \sin(\omega t_1^j) = a_1^j \\ A^j \sin(\omega t_2^j + \psi^j) = b^j \cos(\omega t_2^j) + c^j \sin(\omega t_2^j) = a_2^j \\ A^j \sin(\omega t_3^j + \psi^j) = b^j \cos(\omega t_3^j) + c^j \sin(\omega t_3^j) = a_3^j \end{cases} \qquad (2)$$

from which the maximum amplitude and phase can be obtained by the least square method and where $a_1^j, a_2^j, a_3^j,\ t_1^j, t_2^j, t_3^j$ are given by the BTT measurement process.

The approach described is more appropriate for cases of synchronous excitation which requires the use of at least two probes. In this case a specific probe will capture a blade at the same state of vibration. In (2) it is assumed that the rotation speed is constant when travelling from the first probe to the last one. A criterion can be derived from the angular span of the probes to minimize the maximum amplitude and phase reconstruction error caused by engine acceleration during the measurements.

Another methodology consists in using single-probe measurements for a selected dataset. The advantage of such an approach is the measurement of noise level reduction and the possibility of using single-probe data that avoids the possible errors of the first method possibly stemming from imprecise location of the different sensor positions. Hence the approach can be used to identify mode families (blade bending or torsion) and to place other probes at different locations on the blade tip. Note that the data sampling period should cover a time interval in which the response signal almost reaches steady state. By accepting formulation (1) the system of equations solved by the least-squares method can be written as follows:

$$a^j = b_0^j + \sum_{m=1}^{M} b_m^j \cos \omega_m t + c_m^j \sin \omega_m t \qquad (3)$$

where a^j are the observations made, b_j and c_j are the problem unknowns, and b_0 is the constant offset, particular for each j-th blade; M is the number of frequencies retained in the response.

Additional resources, such as strain gauges, are required to estimate the frequency content of the response. The constant coefficient can be caused by error vibration amplitude calculation a^j where the hypothesis of constant rotation speed during one measurement is accepted. It can also stem from initial displacements of individual blades or a synchronous part in the response.

Fig. 2 illustrates an example of applying the single-probe measurement approach for vibration signal reconstruction. The latter is asynchronous with a sampling frequency of $1/\Omega$, where Ω is the rotation speed.

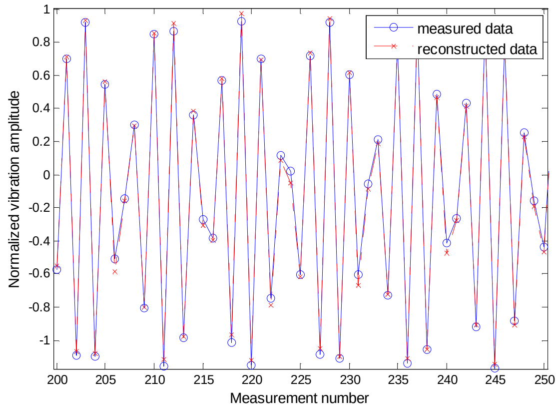

Fig. 2 Reconstruction of blade vibration using single-probe measurements

3. TIP-TIMING MEASUREMENTS

3.1 Experimental setup

The detailed description of the test rig used here is given in [6]. The system mainly consists of one shaft driven inside a vacuum chamber by an electric motor. The test piece investigated was the 36 bladed blisk of a high-pressure compressor stage mounted at end of a shaft (Fig. 3).

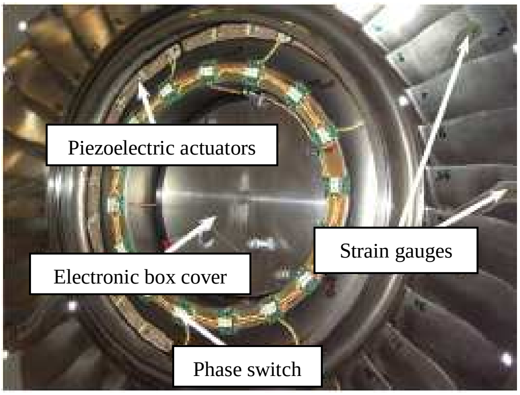

Fig. 3 Instrumented blisk

Excitation was provided by embedded piezoelectric actuators (PZT) driven by power amplifiers through the slip-ring. As described in [6], the distribution of PZTs can be set with 0,1,2 or 4 nodal diameters. Excitation can be standing wave for the disk or travelling wave, using two sets of PZTs with spatial and time relative phase shifts between them. Standing wave excitation was used for all the case studies here. Measurements were taken by strain gauges and transmitted using an inductive telemetry system, and by tip-timing probes. The use of a vacuum chamber (p<10-2 bar) allowed eliminating air-to-structure coupling. The excitation signal was set in terms of frequency, spatial distribution and strength independently of rotation speed, thereby generally producing asynchronous excitation of the blisk.

In Fig. 4 the modes investigated are specified, and are located in areas with low and strong levels of blisk to blade coupling.

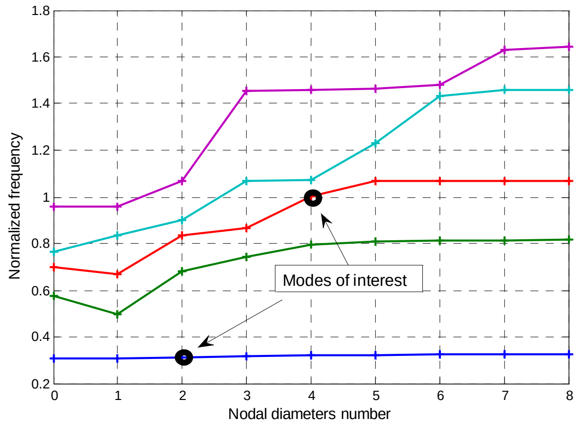

Fig. 4 Frequency vs. number of nodal diameters at rest

3.2 Case study – fixed mode

The mode belonging to family 1F was chosen for mode shape identification in the case of standing wave response (Fig. 5). As mentioned previously, identification can be achieved by using two approaches. Either multi-probe data are used to calculate blade vibration parameters at each measurement (2), or single-probe measurements (3) are performed.

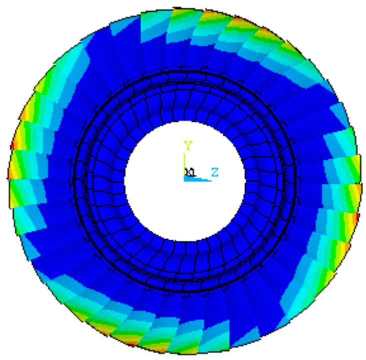

Fig. 5 Computed mode shape 2ND-1 (displacement modulus)

The measurements started with a rotation speed set at Ω=901rmp (sampling frequency of 15.02 Hz). As mentioned previously, the frequency was assumed to be constant during one measurement (when the blade travelled from one probe to another). The experimental setup was characterized by fluctuations of rotation speed of 0.01% from the mean value during the measurements.

The data were delivered by the BTT system with a sampling frequency of 2.5 MHz to approximate each probe impulse. Capacitive probes were used in the setup. Measurements of the mode of interest are shown in Fig. 6 where the sinusoidal excitation is sustained from measurements No. 50 to 800.

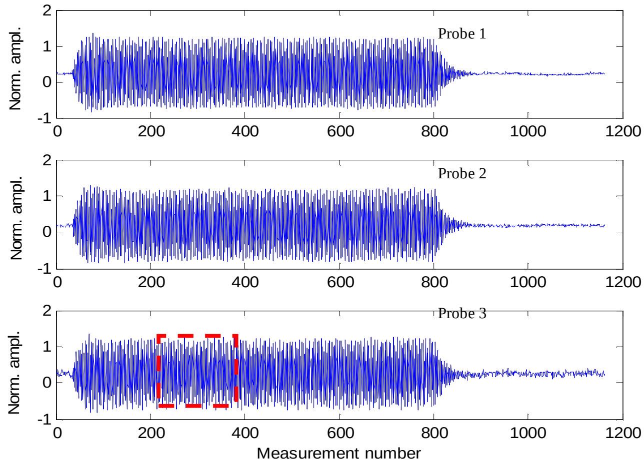

Fig. 6 Tip-timing measurements of standing wave response: Fixed mode 2ND-1 (all probes, blade No.22)

The data from all the probes were then used to calculate the amplitude and phase of blade tip vibration to perform mode shape reconstruction. From Fig. 7 it is possible to identify the response of two nodal diameters. The mode shape can be considered as almost pure, with the exception of a low level of mode distortion due to mistuning or participation by an orthogonal mode. The latter was revealed by the behaviour of certain blades located close to the nodal lines.

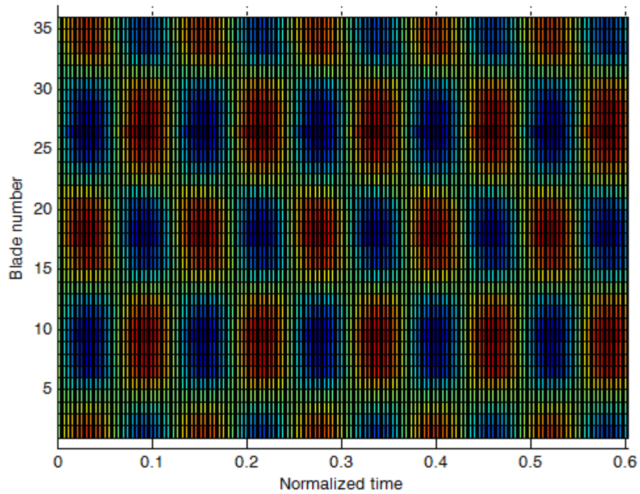

Fig. 7 Mode identification from all probe data: Fixed mode 2ND-1 (measurement No.400)

The same mode shape identification results can be obtained from single-probe data, by selecting the sampling time period covering measurements from 200 to 400 (Fig. 8). Comparison with the strain gauge data is performed qualitatively. The first chart in Fig. 8 shows the distribution of maximum amplitudes with the instrumented blades represented by white bars. Except for blades close to nodal diameters, the phase distribution (0 or +/- 180 deg.) is in very good agreement with a standing wave mode with two nodal diameters.

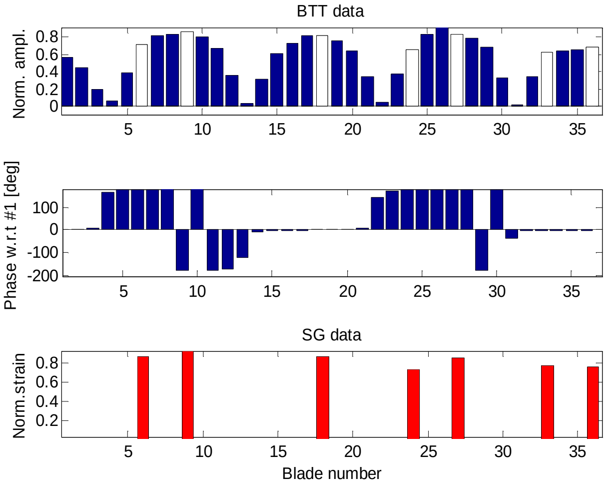

Fig. 8 Mode identification using single-probe measurements: Fixed mode (probe No.2, measurements No.200:400)

3.3 Case study – rotating mode with Coriolis effect

The second case study describes the identification of the mode affected by the Coriolis effect, i.e. leading to mode split and travelling wave response at resonances.

Traditional vibration analysis of cyclic symmetric rotors assumes that the latter are not affected by the gyroscopic effect, or else blisk models specially designed to a generate gyroscopic effect in rotation are used [7], [8]. Normally, such cyclic systems are characterized by pairs of "double" modes with identical natural frequencies with orthogonal mode shapes. Coriolis forces are associated with the blade and disk motion components along axes perpendicular to the axis of rotation. Thus most of modes affected by gyroscopic effect are those with strong participation of the disk, in other words with strong disk to blade coupling. Furthermore, the presence of mistuning should be mentioned as it also results in "double" mode splitting. However, in this case the split ratio in the frequency remains constant and independent of rotation speed, as shown in [6]. Also the confusing similarity between mode splitting due to either mistuning or the Coriolis effect can be solved by analysing the blade vibration phase. In the case of mistuning only, the response at the resonance frequencies will be of standing type, whereas in the case of the Coriolis effect it will be of travelling type at the resonance peaks and for sufficiently split peaks.

The equation of motion in generalized matrix form for an axially symmetric blisk rotating at a constant speed Ω and subjected to Coriolis and centrifugal effects is

$$\mathbf{M}\ddot{\mathbf{q}} + (\mathbf{C} + \mathbf{G}(\Omega))\dot{\mathbf{q}} + (\mathbf{K} + \mathbf{K}_c)\mathbf{q} = \mathbf{f} \,, \qquad (4)$$

where $\mathbf{M}$ is the symmetric mass matrix, $\mathbf{C}$ is the symmetric damping matrix, $\mathbf{G}$ is the skew-symmetric gyroscopic matrix, $\mathbf{K}$ is the symmetric stiffness matrix, $\mathbf{K}_c$ is the stiffness due to stiffening (or softening), $\mathbf{q}$ is the generalized coordinates and $\mathbf{f}$ is a forcing function.

In (4) the gyroscopic matrix is dependent on the frequency of rotation resulting in the split ratio that increases with rotation speed. The presence of split modes in the blisk response has been proven experimentally and numerically [6]. The mode of four modal diameters belonging to the third family (associated with blade mode 2F) was investigated. The strong coupling between disk and blades is revealed by disk ovalization of the deformed blisk shape (Fig. 9).

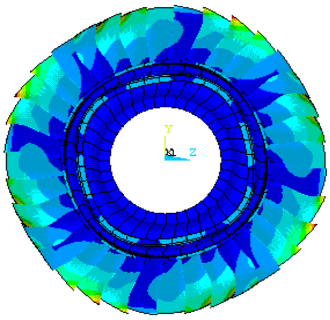

Fig. 9 Computed Mode shape 4ND-3 (displacement modulus)

It should be noted that the blisk is perfectly constrained and its dynamics is not subjected to coupling with the rotor shaft, which was confirmed by the numerical study.

The blisk was run at Ω=1501.4 rpm, producing a sampling frequency of 25.02 Hz for single probe measurements. Data from all the probes were used to reconstruct deformation shapes for two modes: forward mode (Fig. 10a) and backward mode (Fig. 10b). The direction of mode rotation is identified with respect to the direction of blisk rotation. An imperfection of predominantly backward mode can be seen. This event is explained by the participation of standing wave response at the frequency of interest, due to the relatively low rate of mode split for the rotation speed set. It is noteworthy that the summation of the two travelling waves (backward and forward) contains a stationary wave part dependant on the relative amplitudes of the two waves.

By using single-probe measurements, two modes of four nodal diameters can be also identified (Fig. 11a-b). Here, the white bars correspond to the instrumented blades. In comparison to the data obtained from the strain gauge, good qualitative correlation is observed. The strain gauge measurements also confirm the mode distortion revealed by the BTT measurements. If the case of a pure travelling wave response were examined, the magnitudes of maximum amplitudes observed by both strain gauges and tip-timing probes would be very close to each other.

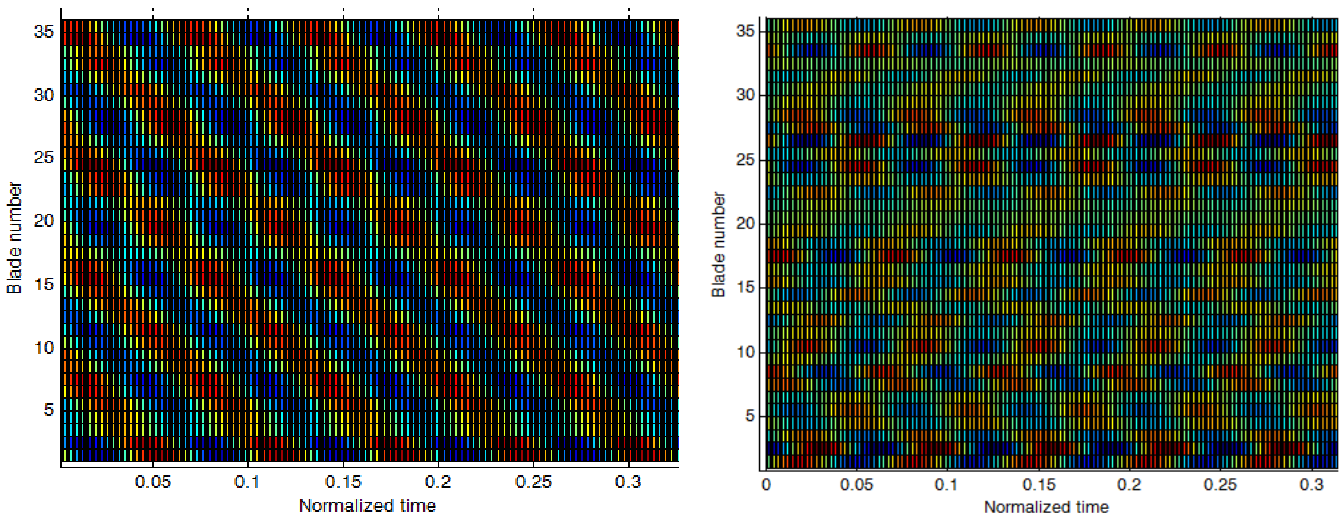

a b

Fig. 10 Mode identification from all probes data (4ND-3): a – forward mode, b – backward mode (measurement No.400)

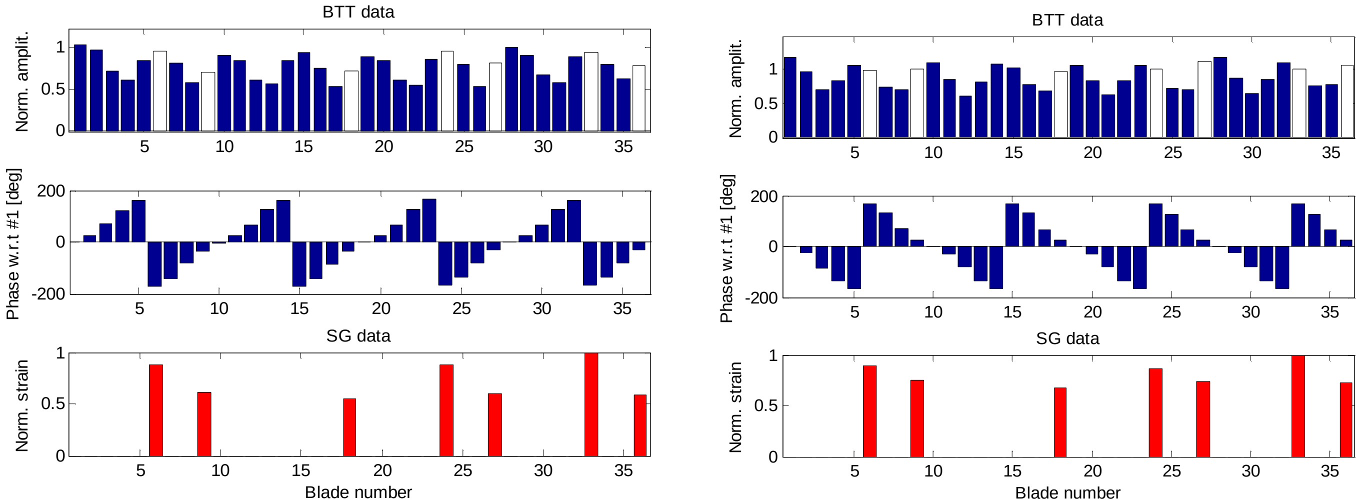

a b

Fig. 11 Mode identification using single-probe measurements (probe No.2, measurements No.200:400): a – forward mode, b – backward mode

4 FORCED RESPONSE RECONSTRUCTION

The completion phase was dedicated to modal damping calculation under rotating conditions. To illustrate this, the mode subjected to the Coriolis effect and producing both forward and backward travelling responses was chosen. To calculate the damping ratio the frequency response was obtained by using seven measurements at different excitation frequencies around both resonances. Then these data were interpolated (Fig. 12) to provide damping ratio calculations using the half power method. Based on the frequency response, mode imperfection can be confirmed once again, notably the presence of the standing wave response reflected by amplitude clustering.

The results of damping ratio calculations using tip-timing data are compared with those obtained from strain gages (7 blades equipped) and shown in Fig. 13. Very good agreement can be seen between both the experimental data obtained with the strain gauges ("SG data") and the tip-timing measurements ("BTT data").

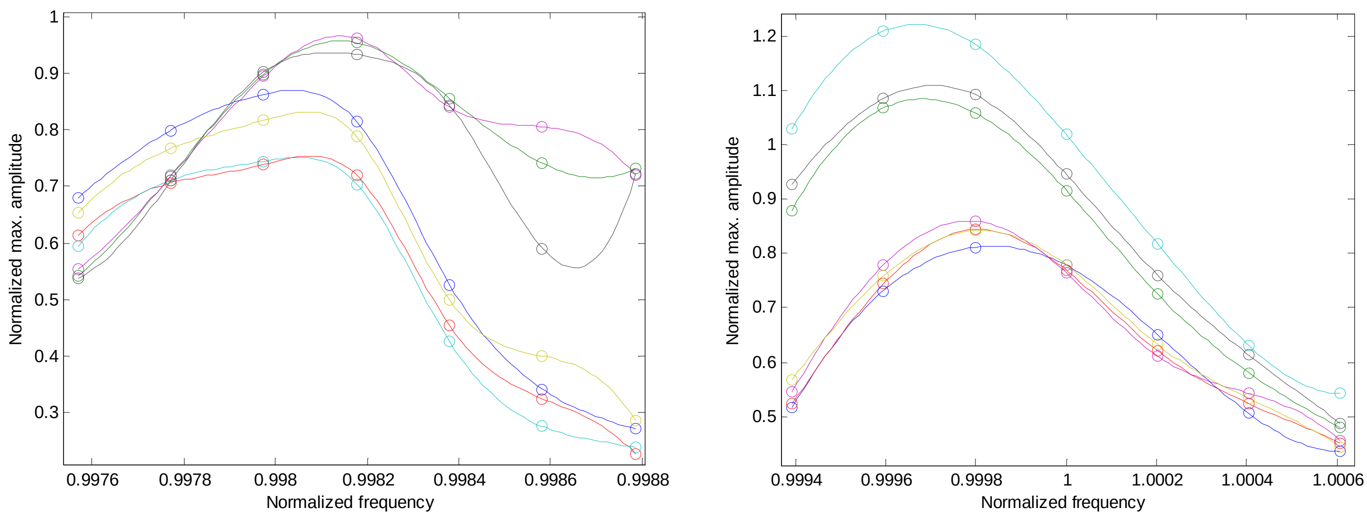

a b

Fig. 12 Frequency response by tip-timing measurement (instrumented blades only): a – forward mode, b – backward mode

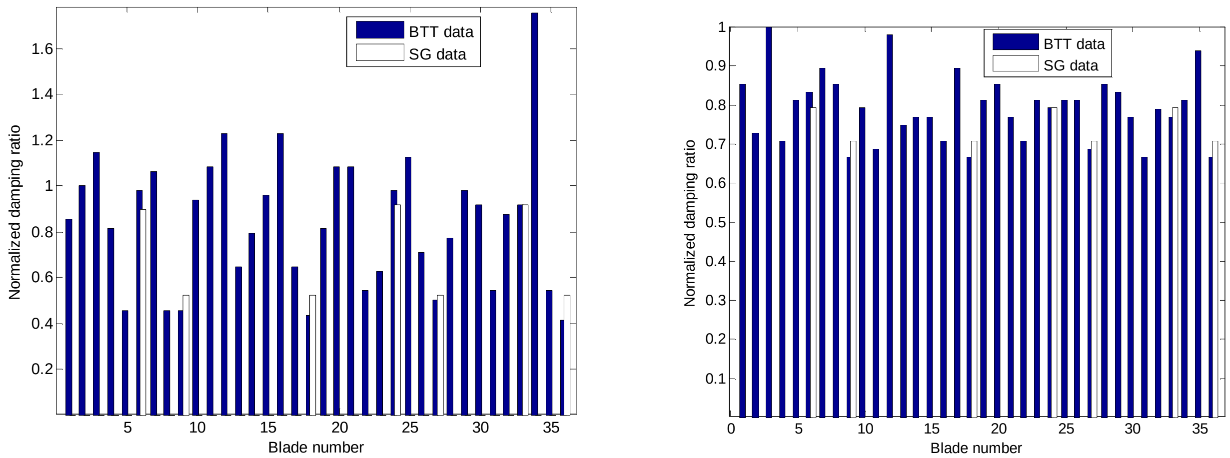

a b

Fig. 13 Identification of modal damping ratio (comparison for instrumented blades only): a – forward mode, b – backward mode

The damping ratio calculated by using individual blades in the case of the backward mode has quasi-uniform distribution oscillating around a normalized damping ratio of 0.79 (Fig. 13b) which can be accepted as the mode damping ratio, whereas the analogous data distribution in the case of the forward mode is far from uniform (Fig. 13a) with the continued presence of the standing wave response or other excited modes. An additional factor influencing mode shape is rotation speed (relatively low under laboratory conditions). It was mentioned previously that the gyroscopic matrix is linear with rotation frequency, thus the mode split and, consequently, mode shape depend on its magnitude.

Two kinds of forced responses are measured by the strain gauges. One with an anti-resonance between the two modes (blades 27, 8, 9, 36 – Fig. 14a) and the other without (blades 24, 6, 33 – Fig. 14b). The value of the damping coefficient of the first (forward) mode identified on blades 24, 6, 33 is probably overestimated by the half power method, whereas blades 27, 8, 9, 36 give a lower value (factor 2). Moreover, the first mode is less responsive than the second (backward). The latter gives identified values with less scattering between blades.

In order to improve these results an identification method using the two modes simultaneously should be applied. The difficulty here is that the BTT measurement process does not provide a phase reference regarding excitation and thus the identification method can only use the amplitude of the response.

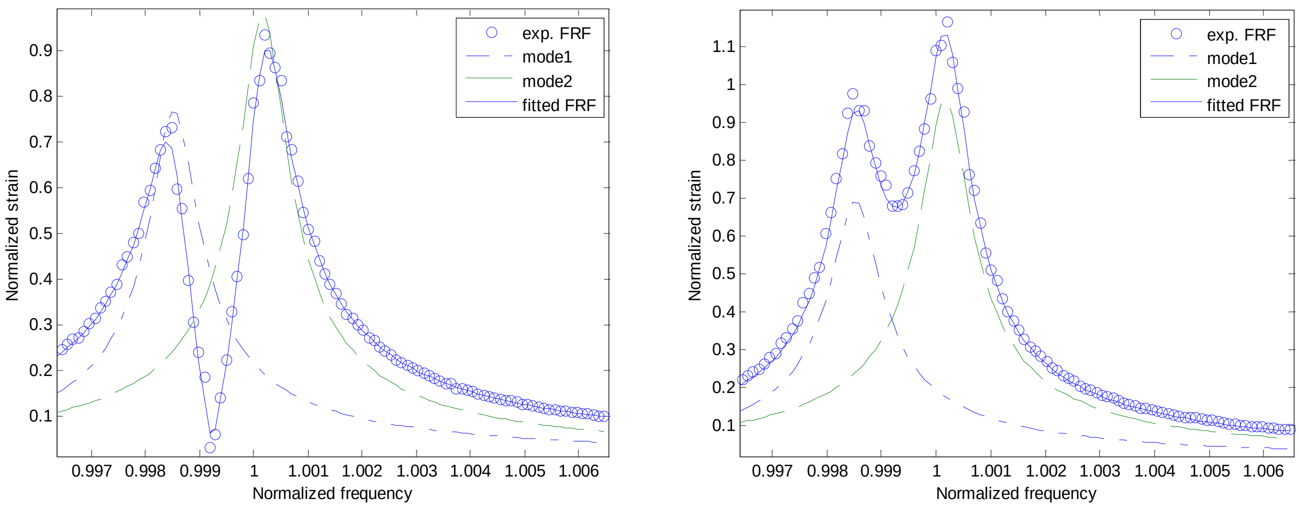

a b

Fig. 14 Frequency response obtained with strain gauges (mode 4ND-3, Ω=1501.4 rpm):
a – response with anti-resonance, b – response without anti-resonance

5 CALIBRATION OF TIP-TIMING RESULTS

In the previous section modal damping obtained after processing tip-timing measurements were compared with data from strain gauges. Here, the correlation of strains obtained by gauges and blade tip tangential displacement obtained from tip-timing data is obtained by using a realistic finite element model of the blisk.

The ratio between vibration amplitude measured by a tip-timing probe and the blade tip vibration amplitude is given in [4]:

$$u_\theta = a_p \frac{\sin\alpha}{\sin\beta}\cos(\beta-\alpha) \qquad (5)$$

where u_θ is the blade tip tangential displacement, a_p is the blade tip displacement seen by the probe p, α is the angle of incidence and β is the angle of displacement vector relating to the incidence (Fig. 15a).

It should be stressed that all the angle data must be taken from the coordinate system tangential to the measurement point, otherwise the correlation results can be considerably modified.

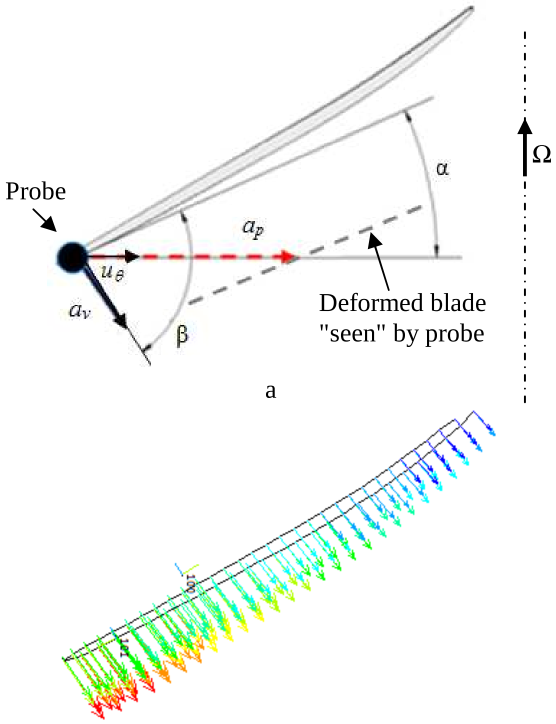

Fig. 15 Relation between BTT measurements and blade tip displacement: a– schematic representation, b – vector plot of blade tip deformation at mode 2ND-2

Using the finite element model, it is possible to link the blade tip tangential displacements and the axial strain transmitted by the strain gauges (Fig. 16) whose direction is radial. In addition the ratio between the experimental blade tip axial displacement obtained by LDV measurement and radial strain εrr at the rest was compared with simulation data using mode 2ND-1 generating the standing wave response (Fig. 5). In this case a good level of correlation was found.

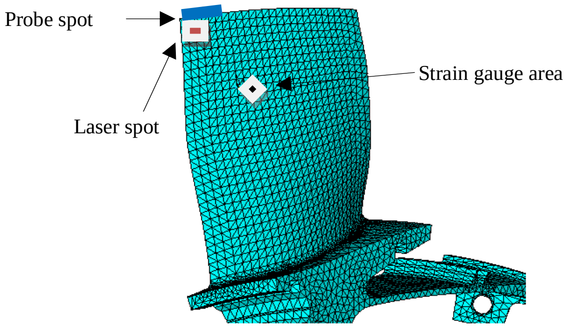

Fig. 16 Experimental measurements on an instrumented blade

The ratio between the blade tip tangential displacement and the blade tip displacement recorded by the probe by using (5) is of the order u_θ / a_p =0.25. By using the finite element model, the ratio between u_θ and ε_{rr} was calculated as of the order 1.5. Then, the ratio of order 5.26 was obtained by comparing the non-normalized BTT data and strain gauge data (Fig. 8). Thus, by using the ratio value 0.25 from (5) and the experimental value of 5.26, the correlation between u_θ and ε_{rr} is of the order 1.31 which correlates well with the finite element model results.

Finally, the correlation results are expressed as follow:

$$R = \frac{K_{FE}}{K_{BTT/SG}} = \frac{(u_\theta/\varepsilon_{rr})_{FE}}{(u_\theta/\varepsilon_{rr})_{BTT/SG}} = \frac{1.5}{1.31} \approx 1.14$$

Obviously, the validation process is influenced by many types of uncertainty, such as the profile deformation curvature at a particular mode, the probe spot diameter exceeding the blade profile thickness and resulting in deformation vector angular position error, the averaging of angle and displacement over the sensor section, the difference of incidence between suction and pressure side, the accuracy of strain calculation by the finite element model, etc.

5 CONCLUSIONS

The study performed allowed the qualitative analysis of phenomena relating to bladed disk dynamics. Compared with conventional measurement techniques, the tip-timing method makes it possible to perform more spatially extended dynamic characterisation of a blisk, a feature that is even more significant for tests of bladed disks that are difficult to access and that have a high number of blades.

The capacity to analyse ODS by tip-timing measurements was demonstrated for both standing wave and travelling wave responses. The latter is challenging due to the modern trend for integral bladed disk design and the need to consider the gyroscopic effect. It was also shown that the effect causes the mode to rotate even in the case of standing wave excitation.

Good conformity of the damping ratio calculation obtained from the forced response of the blisk, obtained by using tip-timing with strain gauge measurements, was demonstrated. Moreover, the validation of the blade tip amplitude calculation from BTT data was performed by correlating strain gauge data with blade tip displacement, which requires a realistic finite element model. It should be noted that due to geometrical effects, prior knowledge of the direction of the displacement vector is needed in order to calibrate BTT data. Also, different factors may affect the accuracy of the derived tip displacement. Additionally, the problem consists in interpreting the tip-timing results at frequencies at which several modes respond.

A single frequency point excitation can be used in view to avoiding frequency response measurement for modal damping calculations which can be time consuming. Consequently, the transient zone of the tip-timing signal corresponding to excitation onset or end may provide the information required. This would dramatically decrease the number of experiments, but with the drawback of having to know the natural frequency with precision.

Another perspective consists of using single-probe measurements to identify a mode belonging to a certain family. This can be performed by placing different probes at the blade tip profile and, thus linking its deformed state with a mode family. Also questions of modal extraction without knowledge of the phase reference by using only BTT data could be considered.

ACKNOWLEDGMENTS

This research was co-funded by the European Commission as part of the 7th Framework Programme (FUTURE project, grant agreement number 213414, [9]).

REFERENCES

[1]. Salhi, B. at al. 2008, Modal parameter identification of mistuned bladed disks using tip timing data. *Journal of Sound and Vibration*, vol. **314** (3-5), pp. 885-906

[2]. Gallego-Garrido, J., Dimitriadis, G., Wright, J. R. 2007, A class of methods for the analysis of blade tip timing data from bladed assemblies undergoing simultaneous resonances – Part I: Theoretical Development. *International Journal of Rotating Machinery*, Vol. **2007**, p.11

[3]. Heath, S., Imregun, M., 1996, "An improved single-parameter tip-timing method for turbomachinery blade vibration measurements using optical laser probes", *International Journal of Mechanical***,** Vol. **38** (10), pp.1047–1058.

[4]. Zielinski, M., Ziller, G., 2000, "Noncontact vibration measurements on compressor rotor blades. *Measurements Science and Technology*, Vol. **11**, Vol. 847–856.

[5]. Kharyton V., Laine J.-P., Thouverez F., Kucher O. Simulation of tip-timing measurements of a cracked bladed disk forced response. *Proceedings of ASME conference "Turboexpo 2010"*, 14-18 June 2010, Glasgow, UK

[6]. Gibert C., Kharyton V., Thouverez F., Jean P. On forced response of a rotating integrally bladed disk: predictions and experience. *Proceedings of ASME conference "Turboexpo 2010"*, 14-18 June 2010, Glasgow, UK

[7]. Nikolic, M., Petrov, E., Ewins, D. 2007, "Coriolis forces in forced response of mistuned bladed disks". Journal of Turbomachinery, Vol. **129**, pp. 730–739.

[8]. Kim, H., Shen, I.Y., 2009, "Ground-Based Vibration Response of a Spinning, Cyclic, Symmetric Rotor With Gyroscopic and Centrifugal Softening Effects". Journal of Vibration and Acoustic, Vol. **131**, pp. 1–13.

[9]. http://www.future-project.eu/

